posited core histone octamers onto circular template DNA with polyglutamic acid at a histone to DNA mass ratio of 0.8, and we purified the resulting chromatin by sucrose gradient centrifugation. We estimated the concentration of the reconstituted chromatin by extraction of the samples with phenol-chloroform, and then by agarose gel electrophoresis and ethidium bromide staining with DNA standards. The purified chromatin was then subjected to salt gradient dialysis from 0.6 M to 0.05 M KCl in the absence or presence of GAL4-VP16 (*18*) with variable amounts of purified histone H1 from *Drosophila* embryos. Except where indicated, GAL4-VP16 was used at a concentration of 1.5 dimers per binding site. The samples were subjected to in vitro transcription analysis with the soluble nuclear fraction [prepared by extraction of nuclei with 0.1 M KCl instead of the previously recommended 0.4 M potassium glutamate (*19*)]. We assayed synthesis of RNA by primer extension analysis, and we quantitated synthesis by liquid scintillation counting of the appropriate gel slices. With different chromatin preparations, we observed some variation in the relative amounts of transcription with the naked DNA templates compared with the nucleosomal templates. This variation was due to inaccuracy in the determination of the concentration of the reconstituted chromatin after sucrose gradient purification and does not affect the conclusions of experiments based on the magnitude of activation by GAL4-VP16.

3. These experiments were designed to provide the GAL4 binding sites either cis or trans to the adenovirus E4 promoter to maintain a constant concentration of GAL4 recognition sites in each reaction. We accomplished this by mixing equimolar amounts of two plasmids in each reaction as follows: the pG5I1300AE4T (with the GAL4 binding sites in the cis configuration) was transcribed in the presence of pUC119, whereas pG0I1300AE4T (which does not contain GAL4 binding sites) was transcribed in the presence of pUC119-G5, which is identical to pUC119, except that it contains five GAL4 binding sites in the polylinker (in the trans configuration to the promoter). When the pG0I1300AE4T template was transcribed as naked DNA in the absence of the pUC119-G5 plasmid, we observed severalfold activation of transcription by GAL4-VP16, presumably because the excess GAL4-VP16 interacted with cryptic, low-affinity sites in the vicinity of the RNA start sites. In contrast, when the pG0I1300AE4T template was transcribed as naked DNA in the presence of the pUC119-G5 plasmid, GAL4-VP16 did not activate transcription (Fig. 1B). With the pG5I1300AE4T template as naked DNA, we did not observe transcriptional activation either with the template alone or with pUC119 (Fig. 1A), probably because the GAL4-VP16 was bound to the GAL4 recognition sequences located 1300 bp upstream of the RNA start site rather than the cryptic GAL4 binding sites. We have also performed transcription experiments with the pG5I1300AE4T template as chromatin in the presence of an equimolar amount of pUC119-G5 and have observed long-range activation of transcription by GAL4-VP16 (*20*).
14. Y.-S. Lin *et al.*, *Cell* **54**, 659 (1988).
15. P. J. Laybourn and J. T. Kadonaga, unpublished data.
16. M. Carey, Y.-S. Lin, M. R. Green, M. Ptashne, *Nature* **345**, 361 (1990).
17. The equation, transcriptional activation = $(1 - c + cf)^N$, was derived as follows. First, to exclude either positive or negative cooperativity of binding, we assumed that the protomers of the activator bind randomly to the template according to a binomial distribution. Then, to enable each factor to activate transcription to its full potential, we assumed the action of each of the activators bound to a single template to be independent and additive in terms of free energy (that is, not cooperative). In this manner, the magnitude of transcription at a template with N factors bound relative to that without any factors bound would be f^N, where f is the amount of transcriptional activation by a single factor bound to a template. Next, we define c as protomers of activator per binding site, where $0 \leq c \leq 1$ (for simplicity, it is assumed that all protomers of activator are bound to the template). It follows that c is the probability that a factor is bound to a given site, whereas $(1 - c)$ is the probability that a factor is not bound to a particular site. Combining these terms, we can describe transcriptional activation as a function of c for $N = 3$, for example, by the following equation: transcriptional activation = $(1 - c)^3 + 3c(1 - c)^2 f + 3c^2(1 - c)f^2 + c^3 f^3$, which can be simplified to $[(1 - c) + cf]^3$. Generalization of this formula for N binding sites gives the equation presented above.
18. I. Sadowski, J. Ma, S. Triezenberg, M. Ptashne, *Nature* **335**, 563 (1988); D. I. Chasman, J. Leatherwood, M. Carey, M. Ptashne, R. D. Kornberg, *Mol. Cell. Biol.* **9**, 4746 (1989); M. Ptashne, *Nature* **335**, 683 (1988).
19. R. T. Kamakaka, C. M. Tyree, J. T. Kadonaga, *Proc. Natl. Acad. Sci. U.S.A.* **88**, 1024 (1991).
20. M. D. Bulger and J. T. Kadonaga, unpublished data.
21. We thank B. Zimm for advice and assistance in the derivation of the equation that describes factor-mediated transcriptional activation in the absence of cooperativity; M. Carey for the gift of pG5I1300AE4T and pG0I1300AE4T; B. Zimm, N. Cozzarelli, M. Botchan, and R. Tjian for ideas and insight regarding possible mechanisms for long-range activation of transcription with chromatin templates; and D. Spector, B. Zimm, R. Kamakaka, G. Croston, M. Bulger, C. Tyree, S. Paranjape, C. George, and L. Kerrigan for improving the quality of this manuscript. J.T.K. is a Lucille P. Markey Scholar in the Biomedical Sciences and a Presidential Faculty Fellow. Supported by grants from NIH, NSF, the Council for Tobacco Research, and the Lucille P. Markey Charitable Trust.

1 May 1992; accepted 20 July 1992

Malignant Transformation by a Mutant of the IFN-Inducible dsRNA-Dependent Protein Kinase

Antonis E. Koromilas, Sophie Roy,* Glen N. Barber, Michael G. Katze, Nahum Sonenberg†

The double-stranded RNA-dependent protein kinase (dsRNA-PK) is thought to be a key mediator of the antiviral and antiproliferative effects of interferons (IFNs). Studies examining the physiological function of the kinase suggest that it participates in cell growth and differentiation by regulating protein synthesis. Autophosphorylation and consequent activation of dsRNA-PK in vitro and in vivo result in phosphorylation of the α subunit of eukaryotic initiation factor–2 (eIF-2) and inhibition of protein synthesis. Expression of a functionally defective mutant of human dsRNA-PK in NIH 3T3 cells resulted in malignant transformation, suggesting that dsRNA-PK may function as a suppressor of cell proliferation and tumorigenesis.

Interferons induce many proteins (*1*), the best characterized of which are the dsRNA-PK (*2*), the 2′-5′ oligoadenylate synthetase, and the Mx protein (*3*). The first two proteins are thought to participate in mediation of the antiviral and antiproliferative effects of IFNs and require dsRNA for their activation (*3*). The dsRNA-PK is a serine-threonine–specific protein kinase and displays two distinct kinase activities: (i) autophosphorylation and (ii) phosphorylation of the α subunit of the eukaryotic translation initiation factor eIF-2 (*4*), a modification that causes inhibition of protein synthesis (*5*).

Complementary DNAs for human (p68) and murine (p65) dsRNA-PKs have been cloned (*6*, *7*), and the corresponding proteins show 61% sequence identity (*7*). The yeast eIF-2 kinase GCN2 (*8*), which is thought to be the homolog of the mammalian dsRNA-PK, displays 38% identity with its human counterpart in the catalytic domains (*9*). Another mammalian eIF-2 kinase, the heme control repressor (HCR), also exhibits sequence identity (42%) with p68 (*10*). All four kinases contain the 11 kinase catalytic domains that are conserved among all protein kinases (*11*). However, p68, p65, and GCN2 exhibit further homology in the region between catalytic domains V and VI (*7*, *8*). This region contains an invariable sequence of six amino acids (Leu-Phe-Ile-Gln-Met-Glu; residues 361 to 366 in p68); in HCR, the sequence Leu-His-Ile-Gln-Met-Gln diverges at two positions. Although its significance is not clear, this common sequence has been suggested to modulate the kinase activity toward eIF-2α and the interaction with effector proteins (*9*).

To investigate the importance of dsRNA-PK in control of cell growth, we attempted to express wild-type (wt) kinase and a mutant kinase, lacking the six conserved amino acids between catalytic domains V and VI (*12*), in NIH 3T3 cells. We reasoned that the conserved sequence

A. E. Koromilas, S. Roy, N. Sonenberg, Department of Biochemistry and McGill Cancer Center, Faculty of Medicine, McGill University, Montreal, Canada H3G 1Y6.
G. N. Barber and M. G. Katze, Department of Microbiology, School of Medicine, University of Washington, Seattle, WA 98195.
*Present address: Department of Microbiology and Immunology, Faculty of Medicine, University of California, San Francisco, CA 94143–0502.
†To whom correspondence should be addressed.

would be critical for the biological function of p68. We chose human dsRNA-PK because its expression can be easily distinguished from that of the endogenous murine kinase with the use of a monoclonal antibody (MAb) specific for the human kinase. We chose NIH 3T3 cells because this cell line has been used successfully to demonstrate the phenotypic effects of a number of proto-oncogenes (*13*). The wt p68 and mutant (p68Δ6) p68 cDNAs were subcloned into the retroviral expression vector pMV7, downstream of the Moloney murine leukemia virus (Mo-MuLV) 5′ long terminal repeat (LTR) (*14*). A pMV7 retroviral construct without the p68 cDNA sequence was used as a control. These constructs were introduced into the amphotrophic packaging cell line DAMP by electroporation (*15*), and recombinant viruses were harvested from G418-resistant cells. NIH 3T3 cells were infected with the recombinant viruses and selected in G418, and drug-resistant colonies were isolated and characterized.

When NIH 3T3 cells were infected with pMV7-p68 retrovirus, no colonies were observed upon G418 selection; in contrast, infection with pMV7 and pMV7-p68Δ6 retroviruses yielded 2644 and 680 colonies, respectively (*16*). One possible explanation for the absence of colonies after infection with pMV7-p68 virus is that expression of wt p68 results in a global inhibition of protein synthesis as a direct consequence of p68 activation by autophosphorylation and the subsequent phosphorylation of eIF-2α. This hypothesis is consistent with the recent demonstration that expression of human dsRNA-PK in yeast cells results in inhibition of cell growth (*9*). We note, however, that certain cell lines, including the DAMP virus packaging cell line, tolerate excess amounts of wt p68 kinase (*17*).

Twenty-seven colonies of NIH 3T3 cells infected with pMV7-p68Δ6 virus were randomly selected, expanded, and examined for morphological changes. Most of these cell clones (17, or 63%) displayed spindle-shaped morphology and increased refractility, indicative of a transformed phenotype (Fig. 1B). Control pMV7-infected cells (cell line NIH 3T3 pMV7-5) had a flat morphology indistinguishable from that of parental NIH 3T3 cells (Fig. 1A). We also examined the growth properties of the transformed clones. The clones showed faster doubling times (by ~15%) and greater saturation densities (increased by ~50%), consistent with their transformed phenotype (Table 1). Furthermore, cells expressing mutant p68Δ6 grew in soft agar (Fig. 1, F and H), whereas NIH 3T3 cells infected with pMV7 did not (Fig. 1, E and G, and Table 1). All nude mice (n = 13) injected with p68Δ6-transformed cells developed tumors within 2 to 4 weeks, whereas animals injected with NIH 3T3 cells infected with pMV7 virus did not develop tumors within the 13 weeks of observation (one mouse out of three developed a tumor after 60 days) (Table 1). Cells from excised tumors retained their ability to grow in medium containing G418 and expressed the mutant p68Δ6 protein.

The concentration of p68 kinase RNA in NIH 3T3 pMV7 and NIH 3T3 pMV7-p68Δ6 clones was determined by Northern analysis of total RNA (Fig. 2A). With a probe derived from human p68 cDNA (6), we observed expression of a 5-kb RNA in all NIH 3T3 pMV7-p68Δ6 clones, but not

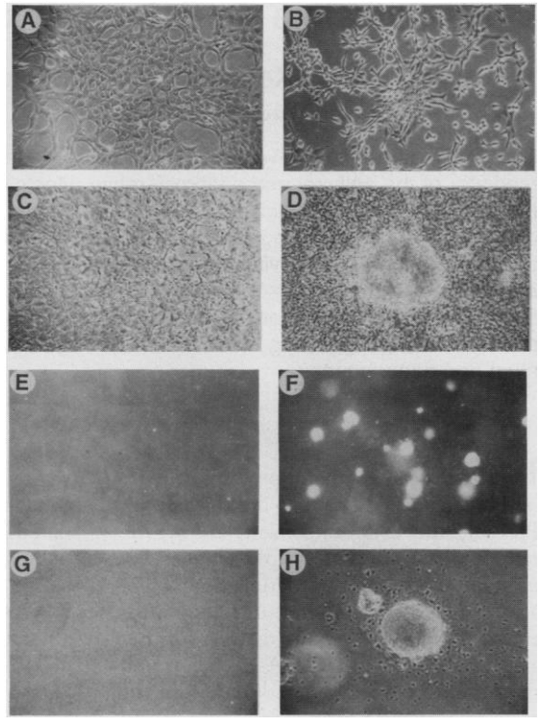

Fig. 1. Morphological characteristics of p68Δ6-expressing cells. Cells from control NIH 3T3 pMV7-5 (A, C, E, and G) and NIH 3T3 p68Δ6-12 (B, D, F, and H) clones were plated at 1 × 10^5 cells per 100-mm dish in DMEM supplemented with 10% heat-inactivated FBS. Culture medium was changed every 3 days. (**A** and **B**) Cells in exponential growth. (**C** and **D**) Cells maintained in culture for 1 week after reaching confluency. (**E** to **H**) Anchorage-independent growth. Cells were plated in soft agar. Optical magnification: ×63 (E and F), ×160 (G and H).

Table 1. Growth properties of cells expressing p68Δ6.

Clone	Growth in monolayers*		Cloning efficiency (%)†	Tumorigenicity‡	
	Doubling time (hours)	Saturation density (10^6 cells)		Animals with tumors/animals injected	Latency (days)
NIH 3T3 pMV7-5	27.2 ± 1.2	3.2 ± 0.3	0	1/3	60
NIH 3T3 pMV7-p68Δ6-1	24.1 ± 0.9	4.2 ± 0.5	10.5 ± 0.2	4/4	24–28
NIH 3T3 pMV7-p68Δ6-2	23.2 ± 1.0	5.0 ± 0.3	24.3 ± 0.4	4/4	22–25
NIH 3T3 pMV7-p68Δ6-3	23.8 ± 0.8	4.7 ± 0.4	15.2 ± 0.3	2/2	26–28
NIH 3T3 pMV7-p68Δ6-12	22.5 ± 0.8	5.8 ± 0.3	31.0 ± 0.1	3/3	15–20

*Measured by seeding 2 × 10^4 cells in 35-mm dishes in DMEM supplemented with 10% fetal bovine serum (FBS). Medium was changed every 3 days. Doubling time was determined by counting cells every 2 days and calculating the growth rate of exponentially growing cells. Saturation density was the number of cells in culture 3 to 4 days after reaching confluency. Numbers are the average of two experiments ± the standard deviation. †Cells (1 × 10^4) were suspended in a 0.35% agar solution in DMEM containing 20% FBS, and overlaid onto a 0.5% agar solution in DMEM containing 20% FBS in 35-mm plates. One day after incubation at 37°C and 5% CO_2, 2 ml of DMEM supplemented with 20% FBS was added. Cells grown in soft agar were counted 2 weeks after plating. Cloning efficiency is the number of colonies × 100 divided by the number of cells plated. Numbers are the average of two experiments. ‡Examined in 4- to 8-week-old athymic mice (CD1 *nu/nu*; Charles River). Cells (1 × 10^6) suspended in 100 μl of PBS were injected subcutaneously on the left side of the lower limb. The time required to produce tumors of at least 3-mm diameter was considered the latency period. Mice were inspected for 90 days.

in NIH 3T3 cells infected with the pMV7 virus. The 5-kb RNA species corresponds to a transcript initiating at the 5′ LTR of the Mo-MuLV and terminating within the 3′ LTR, because the p68 cDNA lacks a polyadenylation site. Endogenous p65 kinase mRNA was not detected in control NIH 3T3 pMV7 cells. The amount of p68Δ6 protein in the various clones was determined by immunoblotting (*18*). A polypeptide of ~68 kD was detected in all transformed clones but not in NIH 3T3 cells infected with pMV7 virus [Fig. 2B and (*17*)].

To investigate the mechanism of transformation by p68Δ6 kinase, we assayed its kinase activity in vitro. Capped wt p68 and p68Δ6 RNAs were transcribed from the T7 promoter (*19*) of the p68-pcDNAI/NEO (*20*) and p68Δ6-pcDNAI/NEO constructs (*12*), and translated in a reticulocyte lysate system (*20*). A MAb to wt p68 (*4*) immunoprecipitated similar amounts of products from both RNAs (*17*). Kinase activity was assayed by p68 autophosphorylation and phosphorylation of exogenously added eIF-2α in the presence of [γ-^{32}P]ATP (adenosine triphosphate). Immunoprecipitated wt p68 kinase became phosphorylated on incubation with heparin, a polyanion that mimics the action of dsRNA on p68 kinase (*21*) (Fig. 3A). In addition, wt p68 kinase phosphorylated eIF-2α when activated by heparin (Fig. 3A). In contrast, p68Δ6 protein neither underwent autophosphorylation nor phosphorylated eIF-2α (Fig. 3A). Similarly, p68Δ6 protein was not autophosphorylated even after incubation with a wide concentration range of reovirus dsRNA (*17*). The loss of p68Δ6 protein autophosphorylation could result from a loss of catalytic activity or an inability to bind to kinase activators (reovirus dsRNA, heparin). However, reovirus dsRNA bound with equal efficiency to both wt p68 and p68Δ6 mutant proteins, as determined by their immunoprecipitation after incubation with [^{32}P]dsRNA (Fig. 3B). Thus, p68Δ6 protein maintains its specific dsRNA binding activity. The Leu-Phe-Ile-Gln-Met-Glu sequence probably contributes directly to the catalytic activity of p68 kinase. We also found that the p68Δ6 protein was inactive as a kinase when expressed in COS-7 cells (*17*).

The mechanism by which p68Δ6 protein transforms NIH 3T3 cells is not clear. One possibility is that the kinase functions as a tumor suppressor, and the mutant p68Δ6 protein is a dominant-negative suppressor of endogenous dsRNA-PK. To determine whether p68Δ6 protein suppresses the activation of the endogenous p65 kinase, we examined the dsRNA-dependent phosphorylation profile of cytoplasmic extracts from a control pMV7-infected NIH 3T3 cell line (NIH 3T3 pMV7-5) and from NIH 3T3 pMV7 p68Δ6-12 cells after treatment with murine IFN-β (*22*). Extracts were incubated with reovirus dsRNA in the presence of [γ-^{32}P]ATP and analyzed by SDS-polyacrylamide gel electrophoresis and autoradiography (Fig. 4A). Incubation of NIH 3T3 pMV7-5 cell extracts with dsRNA resulted in the specific phosphorylation of a 65-kD protein only after IFN-β treatment. This protein, which migrates somewhat faster than the human p68 kinase, is most likely the p65 kinase because its phosphorylation was both dsRNA dependent and IFN inducible and it could be immunoprecipitated with a polyclonal antibody to p68 kinase (*17*). However, p65 was not phosphorylated in NIH 3T3 pMV7 p68Δ6-12 cells, even after IFN-β treatment. The phosphorylation of an ~100-kD polypeptide was reduced in NIH 3T3 pMV7 p68Δ6-12 cells. Thus, p68Δ6 protein may function as a transdominant mutant. This conclusion was supported by cotransfecting p68-pcDNAI/NEO and p68Δ6-pcDNAI/NEO plasmids into COS-7 cells. Expression of wt p68 and p68Δ6 proteins was confirmed by immunoblotting, and both proteins were tested for autophosphorylation after immunoprecipitation and incubation with [γ-^{32}P]ATP in the presence of reovirus dsRNA (Fig. 4B). In mock-transfected

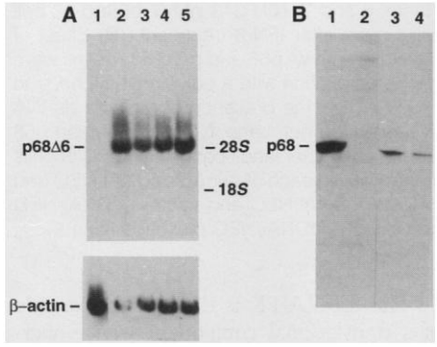

Fig. 2. Expression of p68Δ6 RNA and protein in transfected cells. (**A**) Northern analysis of p68Δ6 RNA. Total RNA was isolated by the guanidinium-thiocyanate method (*36*) from five G418-resistant clones. RNA (20 μg from each clone) was denatured with glyoxal and dimethylsulfoxide, and subjected to electrophoresis on a 1% agarose gel in 10 mM sodium phosphate buffer (pH 7.0) (*37*). RNA was transferred onto a nylon membrane (BioTrans, ICN) and hybridized at 65°C with [α-^{32}P]dATP-labeled random-primed cDNA probes (5 × 10^6 cpm/ml) (*38*) consisting of either the 0.8-kb Eco RI fragment of p68 cDNA (upper panel) or the entire coding sequence of mouse β-actin (lower panel). After hybridization for 16 hours, the filter was washed with 0.1 × SSC [150 mM NaCl and 15 mM sodium citrate (pH 7.0)] plus 1% SDS for 1 hour at 45°C. The filter was dried and exposed to an x-ray film for 10 hours. Lane 1, NIH 3T3 pMV7-5; lane 2, NIH 3T3 pMV7 p68Δ6-1; lane 3, NIH 3T3 pMV7 p68Δ6-2; lane 4, NIH 3T3 pMV7 p68Δ6-3; lane 5, NIH 3T3 pMV7 p68Δ6-12. (**B**) Immunoblot analysis of NIH 3T3 p68Δ6 clones. The blot was prepared as described (*18*). Protein extracts of 293 cells were used as a positive control (lane 1). Lane 2, NIH 3T3 pMV7-5; lane 3, NIH 3T3 pMV7 p68Δ6-3; lane 4, NIH 3T3 pMV7 p68Δ6-1.

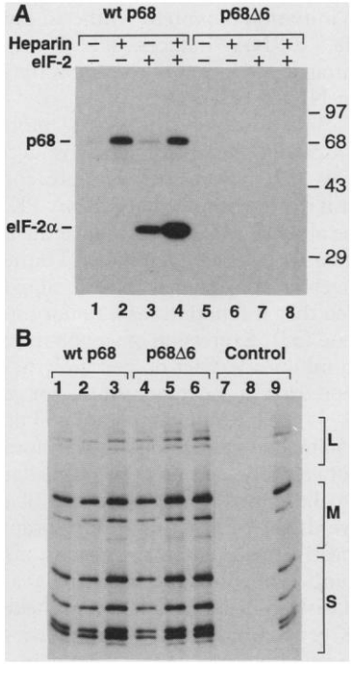

Fig. 3. Functional characterization of p68Δ6 in vitro. (**A**) p68-pcDNAI/NEO (*20*) and p68Δ6-pcDNA/NEO (*12*) plasmids were linearized with Eco RV, and capped transcripts were generated by T7 polymerase in the presence of m^{7}GpppG (*19*). The wt p68 and p68Δ6 proteins were synthesized in vitro in a rabbit reticulocyte system as previously described (*20*). After immunoprecipitation with a MAb to p68 (*4*), proteins were tested for kinase activity (*20*) by incubation with [γ-^{32}P]ATP in the presence (+) or absence (−) of purified eIF-2 (0.5 μg), with heparin (10 U/ml) as activator. Immunoprecipitates were subjected to electrophoresis on an SDS–10% polyacrylamide gel and autoradiography. The positions of molecular mass standards (in kilodaltons) are shown on the right. (**B**) Binding of reovirus dsRNA to wt p68 and p68Δ6 proteins. Equimolar amounts of in vitro translated wt p68 (lanes 1 to 3) and p68Δ6 (lanes 4 to 6), and an equivalent amount of translation mix not programmed with RNA (lanes 7 and 8), were incubated with 5 ng (lanes 1 and 4), 10 ng (lanes 2 and 5), or 25 ng (lanes 3 and 6) of 5′-end-^{32}P-labeled reovirus dsRNA (*20*). The [^{32}P]dsRNA–protein complexes were immunoprecipitated and analyzed on an SDS–10% polyacrylamide gel. Positions of large (L) (~3500 to 3900 nucleotides), medium (M) (~2200 to 2300 nucleotides), and small (S) (~1200 to 1400 nucleotides) reovirus dsRNA species are indicated. Lane 9, 25 ng of [^{32}P]dsRNA loaded directly on the gel.

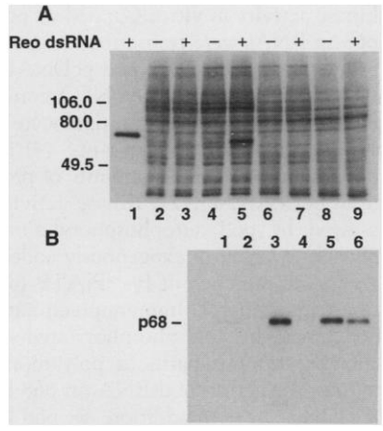

Fig. 4. Evidence that p68Δ6 is a dominant-negative mutant. (**A**) Effect of p68Δ6 protein on endogenous p65 kinase activation in mutant p68Δ6-transformed cells. Subconfluent NIH 3T3 pMV7-5 (lanes 2 to 5) and NIH 3T3 pMV7 p68Δ6-12 (lanes 6 to 9) cells were incubated in the presence of murine IFN-β (1000 IU/ml) (Lee BioMolecular Research Laboratories) for 18 hours. Cell lysates (S10) were prepared as described (*22*). Protein kinase assays contained 10 mM tris-HCl (pH 7.7), 50 mM KCl, 2 mM $MgCl_2$, 5 mM β-mercaptoethanol, [γ-^{32}P]ATP (10 μCi) (Du Pont Biotechnology Systems), 20 μg of S10 extract, and, where indicated, reovirus dsRNA (0.1 μg/ml). Reactions were performed for 30 min at 30°C and terminated by the addition of 2× electrophoresis buffer and boiling. Samples were subjected to electrophoresis on an SDS–8% polyacrylamide gel and autoradiography. Purified human p68 kinase (0.1 μg) was incubated in the assay in place of cell extract (lane 1). Positions of molecular mass standards (in kilodaltons) are shown on the left. Lane 1, pure wt p68; lanes 2 and 3, NIH 3T3 pMV7-5 cell extract; lanes 4 and 5, NIH 3T3 pMV7-5 cell extract after IFN-β treatment; lanes 6 and 7, NIH 3T3 pMV7 p68Δ6-12 cell extract; lanes 8 and 9, NIH 3T3 pMV7 p68Δ6-12 cell extract after IFN-β treatment. (**B**) Effect of p68Δ6 protein on activation of a cotransfected wt p68 kinase. The wt p68 and p68Δ6 proteins were transiently expressed in COS-7 cells (*37*). After immunoprecipitation with a polyclonal antibody to p68 kinase (*39*), the proteins were incubated with [γ-^{32}P]ATP in the presence of reovirus dsRNA (0.1 μg/ml) and electrophoresed on an SDS-8% polyacrylamide gel. Lane 1, purified human p68 kinase (50 ng); lane 2, extract of mock-transfected COS-7 cells. Other lanes contain extracts of cells transfected with 10 μg of p68-pcDNAI/NEO plasmid (lane 3); 5 μg each of p68Δ6-pcDNAI/NEO and vector pcDNAI/NEO plasmids (lane 4), 5 μg each of p68-pcDNAI/NEO and vector pcDNAI/NEO plasmids (lane 5); 5 μg each of p68-pcDNAI/NEO and p68Δ6-pcDNAI/NEO plasmids (lane 6).

cells, no phosphorylation of the endogenous kinase was detected (lane 2). In agreement with the in vitro data, wt p68 became highly phosphorylated upon incubation with dsRNA (lanes 3 and 5), whereas the p68Δ6 kinase was weakly phosphorylated (lane 4). Coexpression of wt p68 and p68Δ6 resulted in a 60% reduction (determined in two separate experiments) in wt p68 autophosphorylation, consistent with a dominant negative effect of the p68Δ6 protein (lane 6).

A transdominant negative action of the mutant p68Δ6 protein is consistent with data indicating that the p68 kinase is probably a dimer of partially phosphorylated subunits and that dimerization is dependent on the phosphorylation state of the subunits (*23*). Phosphorylation of dsRNA-PK is a second-order reaction, whereby two dsRNA-PK molecules bind to one dsRNA molecule, which results in intermolecular phosphorylation (*24*). This mechanism is comparable to transphosphorylation of growth factor receptor tyrosine kinases, a modification that requires prior dimerization of the receptor for subsequent signal transduction (*25*). Indeed, mutations in the catalytic sites of receptor tyrosine kinases have dominant-negative effects (*26*). Thus, we propose that formation of a hybrid wt p68-p68Δ6 dimer results in an inactive kinase. An alternative explanation is that in cells expressing p68Δ6, dsRNA activators are sequestered by the mutant protein, thus preventing the activation of endogenous dsRNA-PK (*27*).

The dsRNA-PK is the second example of a translational component whose aberrant expression can cause malignant transformation, and thus underscores the importance of translational control in regulation of cell growth. Overexpression of eukaryotic initiation factor eIF-4E, the mRNA 5′ cap-binding protein, in NIH 3T3 cells results in malignant transformation (*28*). However, the physiological effect of dsRNA-PK activation may not be limited to initiation of protein synthesis. For example, dsRNA induces IFN-β expression through activation of the transcription factor NF-κB (*29, 30*).

Activation of dsRNA-PK probably is critical for the antiproliferative activity of IFNs (*31, 32*). Other data are consistent with the hypothesis that dsRNA-PK can, in the absence of IFNs, reproduce the antiproliferative effect of IFNs (*9*). The negative effect of p68 on cell growth supports the idea that it functions as a tumor suppressor gene (*33*). Expression of wt p68 in yeast has an inhibitory effect on cell growth, as does expression of the tumor suppressor gene p53 (*9, 34*). Expression of mutant p53 or p68 in mammalian cells results in transformation. Conceivably, certain types of malignancies may be caused by the expression of a defective dsRNA-PK acting in a transdominant negative manner. In this regard, a form of murine lymphoblastic leukemia is associated with an in-frame deletion in the dsRNA-PK gene, which results in expression of an inactive protein (*35*). It remains to be determined whether mutations in dsRNA-PK are associated with malignancies in humans.

REFERENCES AND NOTES

1. S. Pestka, J. A. Langer, K. C. Zoon, C. E. Samuel, *Annu. Rev. Biochem.* **56**, 727 (1987).
2. A. G. Hovanessian, *J. Interferon Res.* **9**, 641 (1989).
3. G. C. Sen and P. Lengyel, *J. Biol. Chem.* **267**, 5017 (1992).
4. J. Galabru and A. G. Hovanessian, *ibid.* **262**, 15538 (1987).
5. R. Jagus, W. Anderson, B. Safer, *Prog. Nucleic Acid Res. Mol. Biol.* **25**, 127 (1981).
6. E. Meurs *et al.*, *Cell* **62**, 379 (1990).
7. G. S. Feng, K. Chong, A. Kumar, B. R. G. Williams, *Proc. Natl. Acad. Sci. U.S.A.* **89**, 5447 (1992).
8. M. Ramirez *et al.*, *Mol. Cell. Biol.* **11**, 3027 (1991); T. E. Dever *et al.*, *Cell* **68**, 585 (1992).
9. K. L. Chong *et al.*, *EMBO J.* **11**, 1553 (1992).
10. J.-J. Chen *et al.*, *Proc. Natl. Acad. Sci. U.S.A.* **88**, 7729 (1991).
11. S. K. Hanks and A. M. Quinn, *Methods Enzymol.* **200**, 38 (1991).
12. The six–amino acid deletion (Leu-Phe-Ile-Gln-Met-Glu) was generated with the M13 in vitro mutagenesis system (Amersham) and the oligonucleotide 5′-GGTCAAAGACTAAGTGCTTCTGT-GATAAAGGGACCTTGG-3′. The p68Δ6 cDNA was subcloned in Bluescript KS (Stratagene) at the Hind III and Bam HI sites of the cDNA, and the mutation was confirmed by sequencing analysis of both strands of the entire cDNA with the dideoxy-chain termination method [F. Sanger, S. Nicklen, A. R. Coulson, *Proc. Natl. Acad. Sci. U.S.A.* **74**, 5463 (1977)]. For p68Δ6-pcDNAI/NEO construction, the p68Δ6 cDNA was subcloned into pcDNAI/NEO (Invitrogen) at the Hind III and Bam HI sites of p68.
13. R. A. Weinberg, *Cancer Res.* **49**, 3713 (1989).
14. Bluescript KS plasmid containing wt p68 (*6*) or p68Δ6 cDNA inserts (*12*) was digested with Pst I, given blunt ends with T4 DNA polymerase, and ligated to Hind III linkers. After Hind III digestion, the 1.8-kb fragments were subcloned into the Hind III site of pMV7 vector [P. T. Kirschmeier *et al.*, *DNA* **7**, 219 (1988)].
15. Plasmid DNA (50 μg) (*14*) was introduced into the amphotrophic packaging cell line DAMP by electroporation [S. Fleury *et al.*, *Cell* **66**, 1037 (1991)]. Cells were selected in Dulbecco's modified Eagle's medium (DMEM) plus 10% fetal bovine serum (FBS) (heat inactivated) and G418 (500 μg/ml) for 2 weeks.
16. Equal numbers of virus-producing DAMP cells were grown in exponential phase in the absence of G418 for 2 days. Culture supernatants were collected, passed through a 0.4-μm filter, and used to infect 1 × 10^5 NIH 3T3 cells in 60-mm petri dishes for 3 hours [in the presence of polybrene (2 μg/ml)]. G418-resistant clones were isolated 2 weeks after selection. Numbers are the average of two experiments.
17. A. E. Koromilas, S. Roy, G. Barber, M. G. Katze, N. Sonenberg, unpublished data.
18. Cells (1 × 10^7) were washed three times with cold phosphate-buffered saline [140 mM NaCl, 15 mM KH_2PO_4 (pH 7.2), and 2.7 mM KCl] and incubated on ice with an equal volume of 2× lysis buffer [2% Triton X-100, 100 mM KCl, 20 mM tris-HCl (pH 7.5), 2 mM dithiothreitol (DTT), 4 mM $MgCl_2$, 0.4 mM phenylmethylsulfonyl fluoride (PMSF), and aprotinin (0.2 mg/ml)]. The lysate was centrifuged at 10,000*g* for 10 min, and portions containing equal amounts of protein were subjected to electrophoresis on an SDS-9% polyacrylamide gel. The separated proteins were transferred to a nitrocellulose membrane (Schleicher & Schuell) in 25 mM tris-HCl (pH 7.5), 190 mM glycine, and 40% (v/v) methanol for 2 hours at 1 A. The filters were first incubated with 5% (w/v) non-fat dried skimmed milk powder in PBS for 1 hour at room temperature and then with PBS containing a mouse MAb to p68 [A. G. Laurent *et al.*, *Proc.*

Natl. Acad. Sci. U.S.A. **82**, 4341 (1985)], 0.5% (v/v) Triton X-100, and 25% FBS for 1 hour. The blot was incubated in 10 ml of PBS containing 10 μCi of ^{125}I-labeled goat antibodies to mouse immunoglobulin G (New England Nuclear) and 0.5% Triton X-100 for 1 hour, followed by exposure to x-ray film for 12 to 16 hours.
19. D. A. Melton *et al.*, *Nucleic Acids Res.* **12**, 7057 (1984).
20. M. G. Katze *et al.*, *Mol. Cell. Biol.* **11**, 5497 (1991).
21. A. G. Hovanessian and J. Galabru, *Eur. J. Biochem.* **167**, 467 (1987).
22. Cells were washed in ice-cold buffer containing 10 mM tris-HCl (pH 7.7), 6 mM $MgCl_2$, 80 mM KCl, 2 mM DTT, 250 mM sucrose, and 0.1 mM EDTA, packed by centrifugation at 600*g* for 5 min, and lysed by the addition of an equal volume of the above buffer containing 0.2% Triton X-100 (*31*). Homogenate was centrifuged at 10,000*g* for 10 min, and the soluble fraction (S10) was stored at −85°C.
23. J. O. Langland and B. L. Jacobs, *J. Biol. Chem.* **267**, 10729 (1992).
24. M. Kostura and M. B. Mathews, *Mol. Cell. Biol.* **9**, 1576 (1989).
25. A. Hammacher *et al.*, *EMBO J.* **8**, 2489 (1989); C.-H. Heldin *et al.*, *J. Biol. Chem.* **264**, 8905 (1989); A. M. Honegger *et al.*, *Mol. Cell. Biol.* **10**, 4035 (1990).
26. D. A. McClain *et al.*, *J. Biol. Chem.* **262**, 14663 (1987); A. Honegger *et al.*, *EMBO J.* **7**, 3053 (1988); A. Kazlauskas and J. A. Cooper, *Cell* **58**, 1121 (1989); A. Honegger *et al.*, *J. Cell Biol.* **110**, 1541 (1990).
27. J. Galabru, M. G. Katze, N. Robert, A. G. Hovanessian, *Eur. J. Biochem.* **178**, 581 (1989).
28. A. Lazaris-Karatzas, K. S. Montine, N. Sonenberg, *Nature* **345**, 544 (1990).
29. K. V. Visvanathan and S. Goodbourn, *EMBO J.* **8**, 1129 (1989); M. J. Lenardo, C.-M. Fan, T. Maniatis, D. Baltimore, *Cell* **57**, 287 (1989); U. Nielsch, S. G. Zimmer, L. E. Babiss, *EMBO J.* **10**, 4169 (1991); L. F. L. Reis *et al.*, *ibid.* **11**, 185 (1992).
30. P. A. Baeuerle, *Biochim. Biophys. Acta* **1072**, 63 (1991).
31. R. Petryshyn, J.-J. Chen, I. M. London, *J. Biol. Chem.* **259**, 14736 (1984); *Proc. Natl. Acad. Sci. U.S.A.* **85**, 1427 (1988).
32. J. Li and R. Petryshyn, *Eur. J. Biochem.* **195**, 41 (1991).
33. R. A. Weinberg, *Science* **254**, 1138 (1991).
34. S. Fields and S. K. Jang, *ibid.* **249**, 1046 (1990).
35. J. G. Bell, personal communication.
36. P. Chomczynski and N. Sacchi, *Anal. Biochem.* **162**, 156 (1987).
37. J. Sambrook, E. F. Fritsch, T. Maniatis, *Molecular Cloning: A Laboratory Manual* (Cold Spring Harbor Laboratory, Cold Spring Harbor, NY, 1989).
38. A. P. Feinberg and B. Vogelstein, *Anal. Biochem.* **132**, 6 (1983).
39. A. G. Laurent, B. Krust, J. Svab, A. G. Hovanessian, *Biochem. Biophys. Res. Comm.* **125**, 1 (1984).
40. We thank A. Hovanessian for pure p68 kinase and the antibodies to human p68 kinase; A. Hovanessian, R. Perez-Bercoff, J. Pelletier, M. Szyf, and A. Veillette for advice and comments on the manuscript; R. Sekaly for providing the amphotrophic cell line; and V. Adkar and M. Wambach for technical assistance. Supported by grants from the National Cancer Institute and Medical Research Council of Canada to N.S., and by NIH grants AI22646 and RR00166 to M.G.K. A.E.K. is a recipient of a long-term postdoctoral fellowship from the Human Frontier Science Programme Organization.

29 April 1992; accepted 4 August 1992

Formation and Activation of a Cyclin E-cdk2 Complex During the G_1 Phase of the Human Cell Cycle

Andrew Koff, Antonio Giordano,* Dipty Desai, Katsumi Yamashita, J. Wade Harper, Stephen Elledge, Takaharu Nishimoto, David O. Morgan, B. Robert Franza, James M. Roberts

Human cyclin E, originally identified on the basis of its ability to function as a G_1 cyclin in budding yeast, associated with a cell cycle–regulated protein kinase in human cells. The cyclin E–associated kinase activity peaked during G_1, before the appearance of cyclin A, and was diminished during exit from the cell cycle after differentiation or serum withdrawal. The major cyclin E–associated kinase in human cells was Cdk2 (cyclin-dependent kinase 2). The abundance of the cyclin E protein and the cyclin E–Cdk2 complex was maximal in G_1 cells. These results provide further evidence that in all eukaryotes assembly of a cyclin-Cdk complex is an important step in the biochemical pathway that controls cell proliferation during G_1.

A major goal in studying the proliferation of eukaryotic cells is to describe the biochemical pathways that regulate progression through the G_1 phase of the cell cycle. Several cyclins have been identified that may function in G_1 regulation in higher eukaryotes. Transcription of the cyclin D gene is induced in murine macrophages in late G_1 by colony-stimulating factor–1 (*1*), and the gene is located at the breakpoint of a chromosomal rearrangement in a human parathyroid tumor (*2*). The genes encoding cyclin C, cyclin D, and cyclin E were discovered by screening human and *Drosophila* cDNA libraries for genes that could complement mutations in the *Saccharomyces cerevisae CLN* genes, which encode G_1 cyclins (*3–5*). In support of a G_1 function for cyclin E it was shown to bind and activate the Cdc2 protein kinase in extracts from human G_1 cells (*3*) and the steady state level of cyclin E mRNA is cell cycle–dependent in human cells and peaks in late G_1 (*5*).

Immunoprecipitates of cyclin E from exponentially growing MANCA cells (a human B cell line) contain a protein kinase (*3*). We examined the activity of the cyclin E–associated kinase during the cell cycle. We used centrifugal elutriation to separate exponentially growing MANCA cells into eight fractions (Fig. 1A). The cyclin E–associated kinase activity was cell cycle dependent. In three separate experiments, the maximal amount of kinase activity was between four and eight times greater than the minimum kinase activity during the cell cycle (Fig. 1B). The peak in kinase activity corresponded to those fractions containing the greatest percentage of late G_1 and early S phase cells. In some experiments we also observed a smaller second peak of cyclin E–associated kinase activity in the fraction containing cells in G_2 and M phases (*6*).

The activity of the cyclin E–associated kinase differed from that of the kinases associated with cyclin A. Monoclonal antibodies to cyclin A (C160) were used to immunoprecipitate cyclin A and its associated proteins from the same cell extracts in which the cyclin E–associated kinase had been measured (Fig. 1C). Cyclin A–associated kinase activity was first detected at the start of S phase (*7, 8*), but it continued to rise throughout S phase and peaked in G_2. The maximal activity of the cyclin A–associated kinase appeared to be approximately five to ten times that of the cyclin E–associated kinase (*6*).

We examined the kinetics with which the cyclin E–associated kinase accumulated during G_1. MANCA cells were synchronized in early G_1 and allowed to progress into S phase (*8*). Entry into S phase was determined both by flow cytometric measurement of nuclear DNA content (Fig. 1D) and by measuring [^{3}H]thymidine incorporation into chromosomal DNA (*6*). The cyclin E–associated kinase activity increased during G_1 and was maximal just as the cells entered S phase (Fig. 1E). The cyclin A–associated kinases appeared after the cyclin E–associated kinase activity; they

A. Koff and J. M. Roberts, Department of Basic Sciences, Fred Hutchinson Cancer Research Center, 1124 Columbia Street, Seattle, WA 98104.
A. Giordano and B. R. Franza, Freeman Laboratory of Cancer Cell Biology, Cold Spring Harbor Laboratory, Cold Spring Harbor, NY 11724.
D. Desai and D. O. Morgan, Department of Physiology, University of California, San Francisco, CA 94143.
K. Yamashita and T. Nishimoto, Department of Molecular Biology, Graduate School of Medical Science, Kyushu University, Fukuoka City 812, Japan.
J. W. Harper and S. Elledge, Verna and Marrs McLean Department of Biochemistry, Baylor College of Medicine, One Baylor Plaza, Houston, TX 77030.

*Present address: Fels Institute for Cancer Research and Molecular Biology, Temple University School of Medicine, Philadelphia, PA 19140.